Pharmacophore

ISSN-2229-5402

Journal home page: http://www.pharmacophorejournal.com

IN SILICO SCREENING FOR NEURORECEPTOR TARGETS AND DERIVATIZATION OF ALKALOIDS FROM *PHAEANTHUS OPHTHALMICUS*

Joyce Gem M. Cañete[1,2]*, Joanna J. Orejola[1], Junie B. Billones[3]

1. ***Department of Pharmaceutical Chemistry, University of the Philippines Manila, Metro Manila, Philippines.***
2. ***College of Pharmacy and Medical Technology, University of San Agustin, Iloilo City, Philippines.***
3. ***Department of Physical Sciences and Mathematics, University of the Philippines Manila, Metro Manila, Philippines.***

ARTICLE INFO

Received:
10 Jul 2022
Received in revised form:
01 Oct 2022
Accepted:
08 Oct 2022
Available online:
28 Oct 2022

Keywords: *Phaeanthus ophthalmicus*, Neuroreceptors, Benzylisoquinoline alkaloids, Molecular docking, Analogs, Autodock

ABSTRACT

Neurological disorders remained the leading cause of long-term disability and the second leading cause of death in 2019, hence there is an urgent need for new neuropharmacological agents. *P. ophthalmicus* is a Philippine medicinal plant with reported antibacterial, antitubercular, and COX-2 inhibitory activities which have recently been attributed to its alkaloids (+)-tetrandrine and limacusine. It also contains phaeantharine, phaeanthine, oxostephanine, and *O*-methyldauricine which are alkaloids with a benzylisoquinoline moiety also present in the known neuroactive drugs papaverine, morphine, and tubocurarine. As of this writing, there have been no investigations into the neuropharmacological uses of these alkaloids yet. Therefore, extensive molecular docking studies using Discovery Studio software were conducted. Our findings identified 4MF3 (Kainate 1), 5O8F and 6HUK (GABAA), and 6G79 (Serotonin 1B) as potential neuroreceptor targets, which are involved with pain, migraine, stroke, epilepsy, and anxiety, among other neurological disorders. Furthermore, 50 out of 232 generated analogs of the alkaloids displayed better docking scores, novelty, and predicted drug-likeness. It was observed that the replacement of the methoxy groups attached to the bisbenzylisoquinoline moiety generally resulted in better binding. Lastly, a particular corydaldine analog is considered a very promising oral neuropharmacological agent after displaying consistent top docking scores across all neuroreceptors, drug-likeness, and favorable pK *profiles in silico*. Therefore, synthesis of such analog and follow-up *in vitro-in vivo* studies are highly suggested by the researchers.

To Cite This Article: Cañete JGM, Orejola JJ, Billones JB. *In Silico* Screening for Neuroreceptor Targets and Derivatization of Alkaloids from *Phaeanthus Ophthalmicus*. Pharmacophore. 2022;13(5):27-43. https://doi.org/10.51847/Iwm8OUzkbP

Introduction

In 2019, neurological disorders remained the leading cause of long-term disability and the second leading cause of death after heart disease. This group of diseases includes stroke, Alzheimer's disease, other dementias, Parkinson's disease, idiopathic epilepsy, migraine, tension-type headache, motor neuron disease, and others. As a result, there is an increasing need for treatment, rehabilitation, and support services for neurological disorders [1, 2].

Phaeanthus ophthalmicus (Roxb. ex G.Don) J.Sinclair or "kalimatas" is a Philippine medicinal plant documented to treat bacterial conjunctivitis, wounds, and ulcers [3, 4]. These ethnomedicinal uses were later attributed to the alkaloids (+)-tetrandrine and limacusine which were reported to have antibacterial and COX-2 inhibitory activities [4]. Similarly, these alkaloids were reported to be cytotoxic against HeLa cells, while limacusine displayed an additional antitubercular activity *in vitro* and *in silico* [5].

P. ophthalmicus also contains the alkaloids phaeantharine, phaeanthine, oxostephanine, *O*-methyldauricine which have a structural similarity to neuro-active drugs papaverine, morphine, and tubocurarine. They all contain the benzylisoquinoline moiety **(Figure 1)** known to act on the receptors in the nervous system [6, 7].

Corresponding Author: Joyce Gem M. Cañete; Department of Pharmaceutical Chemistry, University of the Philippines Manila, Metro Manila, Philippines. E-mail: jmcanete1@up.edu.ph.

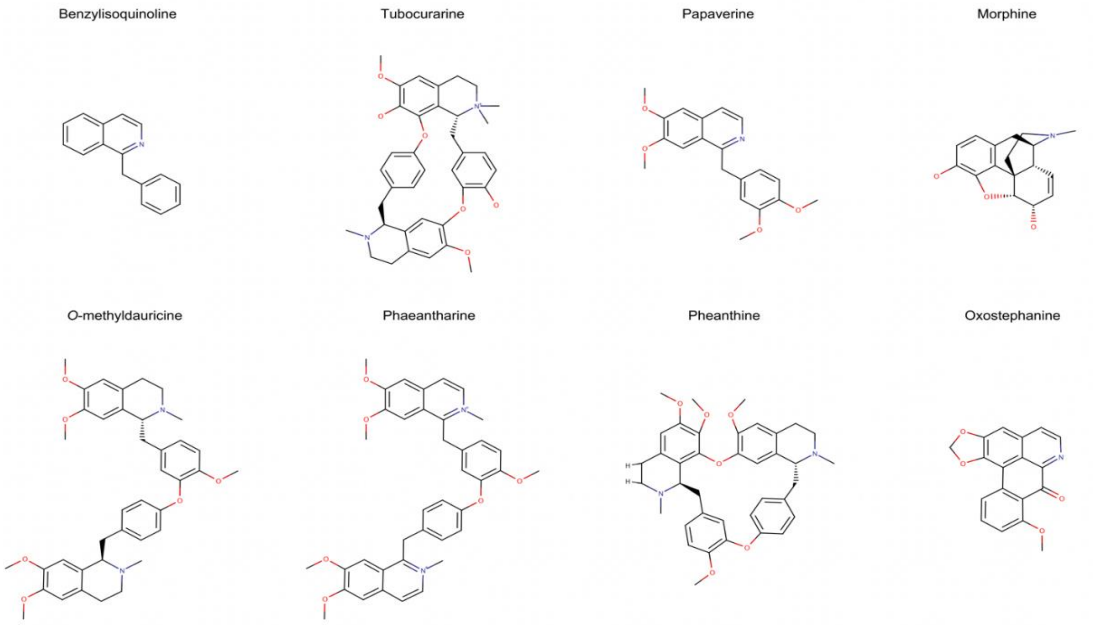

Figure 1. (Top) The benzylisoquinoline moiety is common among the known neuroactive drugs tubocurarine, papaverine, and morphine. (Bottom) *P. ophthalmicus* alkaloids share this structure similarity which makes them interesting drug candidates for targeting the nervous system.

Molecular docking is a widely accepted tool for drug discovery and drug repurposing where new indications for existing drug candidates could be explored at a lower cost similar to high-performance biological screening [8]. On the other hand, *in silico* derivatization has been carried out to produce analogs better than the parent compounds in terms of potency, pharmacokinetic profiles, and other physicochemical properties [9]. Scientific evidence shows that predictions from *in silico* research are comparable with *in vitro* and *in vivo* results [10].

Given the demand for medications that treat or manage neurological diseases, this study investigated the potential neuroreceptor targets of the known alkaloids of *P. ophthalmicus* using molecular docking. Furthermore, *in silico* analogs of alkaloids were prepared, and their binding energies, pharmacokinetic properties, and drug-likeness were compared with the parent compounds.

Materials and Methods

Docking tests were performed using Biovia Discovery Studio (DS) Client v2.5 (Dassault Systèmes) and LigandScout with Autodock as the backend. The crystallographic data files of the targets **(Table 1)** were retrieved from the Research Collaboratory for Structural Bioinformatics (RCSB) Protein Data Bank (PDB) website: www.rcsb.org (accessed on 15 January 2020). The structures of the ligands were downloaded from the PubChem database: https://PubChem.ncbi.nlm.nih.gov (accessed 15 January 2020). The DockRMSD tool (Bell & Zhang, 2019) from https://zhanggroup.org/DockRMSD/ (accessed on 16 January 2020) was used to calculate the RMSD value between the native and experimental poses of the co-crystallized ligand. The novelty of the generated analogs was checked by searching for entries in the following databases: PubChem (https://PubChem.ncbi.nlm.nih.gov), ChemSpider (https://www.chemspider.com/Search.aspx), E-molecules (https://www.emolecules.com), and ChemSynthesis (https://www.chemsynthesis.com).

Table 1. PDB structures screened for molecular docking studies

PDB Code	Description
DOPAMINE RECEPTOR	
6CM4	Human Dopamine 2 Receptor
3PBL	Human Dopamine 3 Receptor
5WIU, 5WIV	Human Dopamine 4 Receptor
GABA RECEPTOR	
4COF	Human β3 homopentamer GABA A
6HUG, 6HUJ, 6HUK, 6HUO, 6HUP	Human α1β3γ2L GABA A
6A96	Human α5β3 GABA A
5O8F	Human chimeric α5β3 GABA A
6DW0, 6DW1	Rat α1β1γ2S GABA A
4MS4, 4MR8, 4MS1	Extracellular domain (ECD) of Human GABA B 1 and 2 subunits
HISTAMINE RECEPTOR	

3RZE	Human histamine 1
MUSCARINIC ACETYLCHOLINE RECEPTOR	
5CXV, 6OIJ	Human muscarinic 1
3UON, 4MQS, 4MQT, 5YC8, 5ZK3, 5ZKB, 5ZKC	Human muscarinic 2
4DAJ, 5ZHP, 4U14, 4U15, 4U16	Rat muscarinic 3
5DSG	Human muscarinic 4
6OL9	Human muscarinic 5
SEROTONIN RECEPTOR	
6G79, 5V54	Human 5-HT 1B
5TVN, 6DRX, 6DRY	Human 5-HT 2B
6A93, 6A94	Human 5-HT 2A
6DG7, 6DG8	Human 5-HT 3A
6NP0, 6HIN, 6HIO, 6HIQ, 6HIS	Mouse 5-HT 3A
NICOTINIC ACETYLCHOLINE RECEPTOR	
5KXI, 6CNK	Human α4β2
6PV7, 6PV8	Human α3β4
3SQ6, 3SQ9	Ligand Binding Domain (LBD) of α7 pentameric
4UXU	ECD of Human α9
5FJV	ECD of Human α2
IONOTROPIC GLUTAMATE RECEPTOR	
2ZNT, 3FVG, 3FVO	LBD of Human iGluR5
3QXM	LBD of Human iGluR6
4MF3	Human GRIK1
5KC8, 5KCA	Amino Terminal Domain (ATD) of iGluR Delta 2
4KCD	Rat/E. coli GluN3A
5EWL, 5EWM	ATD of Xenopus/Human GluN1/GluN2B
5KCJ, 5TP0, 5H8F, 5H8Q	Human GluN1/GluN2A
6E7R, 6E7U	ATD of Rat/Xenopus of GluN1B-GluN2B
METABOTROPIC GLUTAMATE RECEPTOR	
3KS9, 4OR2	Human mGLuR1
5CNI, 5CNJ, 5KZQ	Human mGLuR2
5CNK, 5CNM, 6B7H	Human mGluR3
3LMK, 6FFI, 6N51	Human mGluR5
3MQ4	Human mGluR7
6BSZ, 6BT5, 6E5V	Human mGluR8
4XAQ	ECD of Human mGluR2
4XAR	ECD of Human mGluR3

Screening for Neuroreceptor Targets Using Discovery Studio

The general method for molecular docking was adopted from the paper of Billones and Bangalan [11]. After removing the co-crystallized ligand and unnecessary water molecules and ions, the proteins were prepared using Prepare Protein tool. Minimization protocol was then used to obtain the lowest energy conformation of the prepared protein followed by Align and Superimpose tool before the RMSD was calculated. The protein was defined as the receptor using the Define Selected Molecule as Receptor tool in DS. The location of the co-crystallized ligand was used to generate an active site sphere using Define Sphere from Selection tool. To further optimize the size and coordinates of the site sphere in this study, amino residues within 4 Å around the bound ligand were displayed and the size and location of the site sphere were adjusted to include all the key binding residues as reported in the literature. Self-docking was performed to ensure the reproducibility of the method with an acceptable RMSD value of ≤ 2 Å between native and experimental poses [12, 13]. Using the Prepare Ligands protocol, the compounds were prepared by removing duplicates, varying the ionization based on pH (6.5 to 8.5), enumerating tautomers (retained aromaticity) and isomers, and generating 3D conformations. The Lipinski filter was turned off.

Molecular docking was done using the Dock Ligands (CDOCKER) protocol which is a grid-based molecular docking method based on CHARMm [12]. The target-ligand complexes were evaluated and ranked by calculating their binding energies using the Calculate Binding Energies protocol with *In Situ* Ligand Minimization. Post-analysis of ligand-receptor interactions was carried out using Biovia DS Visualizer 2020 to reveal the unsatisfied bonds within the ligand (i.e., atoms that do not participate in the binding interaction).

Preparation of Analogs of P. Ophthalmicus Alkaloids

Molecular replacements were determined using a combination of literature search and the SwissBioisostere tool from http://www.swissbioisostere.ch (accessed on 5 July 2021). SwissBioisostere's Query Database generates a list of available molecular replacements with data on activity levels, and frequency of use in past research, among other information [14]. This knowledge is useful when modifying small molecules to possibly improve affinity or to circumvent a pharmacodynamics/ pharmacokinetics (pD/pK) issue. Fragment replacements of central cores and modification of peripheral groups within a

compound can efficiently support lead optimization efforts [15]. The 2D structures of the *P. ophthalmicus* alkaloids and their analogs were constructed using MarvinSketch software, cleaned in 3D, and imported as SDF files to LigandScout for docking.

Molecular Docking of the Analogs Using LigandScout (Autodock)

The docking protocol described in LigandScout's User Manual Tutorial Card 13 available from http://www.inteligand.com/ligandscout3/downloads/ligandscout-manual-2010-04-15.pdf (accessed on 3 July 2021) was carried out.

The protein structures were inserted into the structure-based window and the binding site occupied by the co-crystallized ligand was selected. All test ligands were inputted as SDF files, selected, and docked using Autodock 4.2 with the default settings: Genetic algorithm runs = 25, RMSD cluster tolerance = 2 Å, Number of individuals in populations = 150, max number of energy evaluations = 2,500,000, max number of generations = 27,000, exhaustiveness = 8, max number of modes = 9, and max energy differences = 3.

Drug-Likeliness and ADME Prediction of P. Ophthalmicus Alkaloid Analogs

SwissADME http://www.swissadme.ch/ (accessed on 18 August 2021) is an online tool that predicts the physicochemical properties, pK, drug-like nature, and medicinal chemistry friendliness of one or multiple small molecules to support drug discovery [15]. The 3D structures of the analogs were inserted in the Marvin JS window creating their corresponding SMILES, and the 'run' button was clicked to calculate the MLogP values, pK, and drug-likeness scores (Lipinski filter).

Results and Discussion

Screening for Neuroreceptor Targets of P. Ophthalmicus Alkaloids

Cross-docking is a common practice in which novel or test ligands are docked in a binding site occupied by a previously reported molecule (also known as a co-crystallized or native ligand). One of the ways to ensure its reliability is to initially do self-docking where the ligand-receptor complex is reconstructed by docking the native ligand (NL) in its crystal structure receptor. RMSD values of ≤ 2 Å correspond to a good docking solution where the conformation of the ligand that is inside the crystallographic structure can be replicated [13]. Docking scores are based on binding energy, where a higher negative value indicates a better potency [10].

In this study, the neuroreceptors were considered potential targets if the majority of the test ligands (TL) displayed a better docking score than the NL. The results revealed that the top potential neuroreceptors for the TLs are 6G79 (5-HT_{1B}), 6HUK (Human $\alpha1\beta3\gamma2$L $GABA_A$), 5O8F (Human Chimeric $\alpha5\beta3$ $GABA_A$), and 4MF3 (Human iGluR5).

Interestingly, the majority of the TLs did not bind to 6HUO and 6HUP which are also human $\alpha1\beta3\gamma2$L $GABA_A$ receptors. The NLs of 6HUO and 6HUP are the benzodiazepines alprazolam and diazepam (positive allosteric modulators; PAMs), respectively, while 6HUK's NL is bicuculline (a competitive antagonist) [16]. This may indicate that the TLs function as competitive antagonists and not as PAMs. The TLs interacted with more amino acid residues in the active site sphere than the NLs, mainly via H-bonding and hydrophobic bonding **(Table 2)**.

Table 2. Favorable interactions between target neuroreceptors and native ligand/test ligands

Receptor-Ligand pair	Favorable non-covalent bond interactions	Total count
6G79		
EP5 (NL)	2 HB/EB; 1 EB; 2 H-bond; 9 hydrophobic	14
PTR	4 EB; 4 H-bond; 16 hydrophobic	24
OMD	1 HB/EB; 11 H-bond; 11 hydrophobic	23
6HUK		
H0Z (NL)	1 EB; 3 H-bond; 6 hydrophobic	10
LMN	2 HB/EB; 2 EB; 4 H-bond; 11 hydrophobic	19
PTN	1 EB; 6 H-bond; 11 hydrophobic	18
5O8F		
P9N (NL)	2 H-bond; 10 hydrophobic	12
LMN	5 H-bond; 9 hydrophobic	14
OMD	1 EB; 11 hydrophobic	12
OSN	5 H-bond; 8 hydrophobic	13
4MF3		
SXI (NL)	1 HB/EB; 1 EB; 7 H-bond; 3 hydrophobic	12
LMN	1 HB/EB; 2 EB; 6 H-bond; 4 hydrophobic	13
OMD	1 HB/EB; 3 EB; 4 H-bond; 4 hydrophobic	12

PTN	1 HB/EB, 1 EB; 3 H-bond; 3 hydrophobic	8
	**Unfavorable bond – PTN's N7 (positive) with Lys61's N (positive)*	

Note. NL = Native ligand; HB (also H-bond) = hydrogen bond; EB - electrostatic bond; hydrophobic = hydrophobic bond

The higher docking scores and a greater number of favorable non-covalent bond interactions suggest that there is a stronger geometric complementarity between the TLs and the binding site. Therefore, the TLs are predicted to have better activity than the native ligand agonist donitriptan (EP5) in 5-HT_{1B}, competitive antagonist (+)-Bicuculline (H0Z) in $\alpha1\beta3\gamma2L$ $GABA_A$, modulator Pregnanolone (P9N) in $\alpha5\beta3$ $GABA_A$, and antagonist Dasolampanel (SXI) in iGluR5.

Designing Analogs of P. Opthalmicus Alkaloids

In this study, ligand modification was performed to improve *in silico* binding activity since it is known that classical and nonclassical bioisosteric replacements can significantly alter the biological properties of compounds. It is also a routine practice for lead optimization [17, 18].

A comprehensive literature search on common bioisosteres and the use of the SwissBioisostere tool allowed the researchers to pool molecular replacements that are knowledge-based. For the latter, substructure candidates were limited to the first 25 results with the highest frequency and highest # Better (a measure of the bioactivity increase of a given compound) based on drug design optimizations of past research [14, 17].

The other structures were rejected since most of them are bulkier fragments that can adversely affect ADME (e.g., aromatic rings decrease solubility) and can pose a problem when a ligand tries to dock inside a small cavity (i.e., steric clash). For relevance, the results were also further narrowed down to include substructures reported to improve and/or retain the bioactivity of the parent compounds against 5-HT_{1B}, Kainate 1, and GABA alpha subunit only.

Post-docking analysis of the ligand-receptor interactions revealed the unsatisfied bonds (UBs) which include hydrogen bond donor, hydrogen bond acceptor, and charged atoms that did not participate in the interactions as calculated by the software DS Visualizer. A total of 232 analogs were generated **(Table 3)** by replacing the UBs with the pooled bioisosteres in different combinations. In this paper, the analogs are assigned with a subscript "A" (CDN_A, LMN_A, OMD_A, OSN_A, PTR_A, PTN_A) to denote which alkaloid they represent.

Table 3. Analogs of *P. ophthalmicus* alkaloids

Structures of novel strong-binding CDN analogs of *P. ophthalmicus* alkaloids

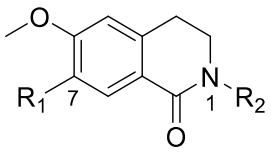

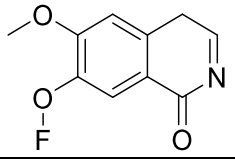

	R_1	R_2	MlogP		MlogP
CDN	OCH_3	H	0.85	**10**	1.03
1	F	OH	1.52		
2	$C(CH_3)_2$	CH_3	2.25		
3	$C(CH_3)_2$	OH	1.95		
4	OCH_3	OH	0.83		
5	CH_3	OH	1.40		
6	OCl	H	0.85		
7	OCl	OH	0.83		
8	OF	H	0.71		
9	OF	OH	0.69		
11	OF	CH_3	0.99		
12	OH	OH	0.54		
13		H	0.86		

Structures of novel strong-binding LMN analogs of *P. ophthalmicus* alkaloids

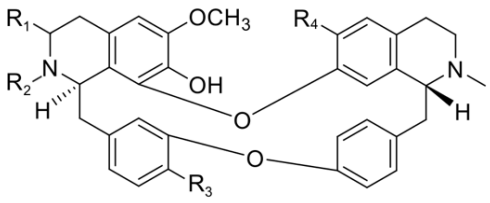

	R_1	R_2	R_3	R_4	MlogP
LMN	H_2	CH_3	OCH_3	OCH_3	3.55

14	OH	CH_2OH	CH_3	$C(CH_3)_2$	3.77
15	H_2	CH_3	OCl	OCH_3	3.55

Structures of novel strong-binding OMD analogs of *P. ophthalmicus* alkaloids

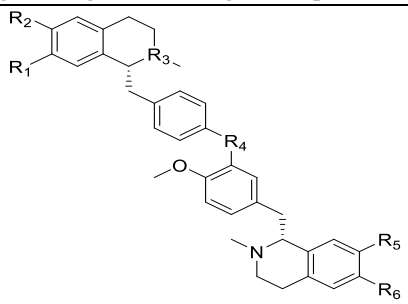

	R_1	R_2	R_3	R_4	R_5	R_6	MlogP
OMD	OCH_3	OCH_3	N	O	OCH_3	OCH_3	3.63
16	NCH_3	OCH_3		CH_2	H		4.25
17	H		N	NH	OCH_3	OCH_3	3.88

Structures of novel strong-binding OSN analogs of *P. ophthalmicus* alkaloids

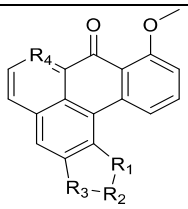

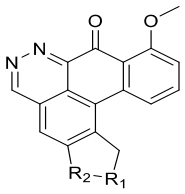

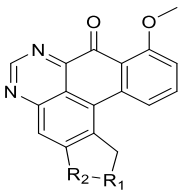

	R_1	R_2	R_3	R_4	MlogP		R_1	R_2	MlogP		R_1	R_2	MlogP
OSN	O	CH_2	O	N	1.39	**33**	NCH_3	CH_2	1.35	**39**	NCH_3	CH_2	1.35
18	O	CH_2	O	O	1.50	**34**	NH	CH_2	1.12	**40**	NH	CH_2	1.26
19	CH_2	O	CH_2	O	1.62	**35**	S	NH	1.15	**41**	S	NH	1.29
20	N	CH=	S	O	1.77	**36**	O	NH	1.15	**42**	O	NH	1.29
21	CH_2	S	CH_2	O	2.47	**37**	O	CH_2	1.12	**43**	O	CH_2	1.26
22	S	CH_2	S	O	2.77	**38**	NCH_3	NH	1.39	**44**	NCH_3	NH	1.39
23	O	CH_2	O	-S-	2.33								
24	CH_2	O	CH_2	CH_3N^+	1.73								
25	S	CH=	N	CH_3N^+	1.90								
26	CH_2	S	CH_2	CH_3N^+	2.58								
27	CH_2	NCH_3	CH_2	N	1.73								
28	CH_2	NH	CH_2	N	1.51								
29	CH_2	NCH_3	NH	N	1.76								
30	CH_2	S	NH	N	1.54								
31	CH_2	O	NH	N	1.52								
32	CH_2	O	CH_2	N	1.51								

Structures of novel strong-binding PTN analogs of *P. ophthalmicus* alkaloids

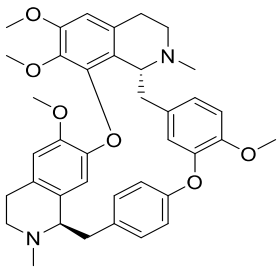

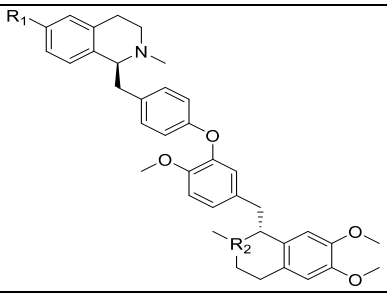

Phaeanthine (PTN)	R_1	R_2	MlogP

MlogP = 3.73 *PTN analogs **45-47** were devoid of ether bridge between their tetrahydroisoquinoline rings*	**45**	$NHCH_3$		3.91
	46		N	3.88
	47	OCH_3	N	3.98

Structures of novel strong-binding PTR analogs of *P. ophthalmicus* alkaloids

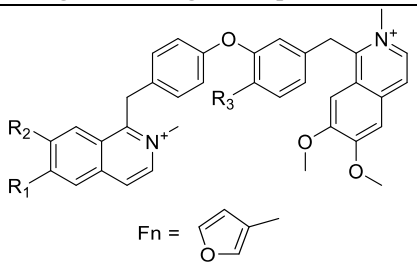

	R1	R2	R3	MlogP
PTR	OCH_3	OCH_3	OCH_3	3.29
48	OCH_3	OCH_3	CH_3	3.81
49	Fn	OCH_3	OF	3.29
50	Fn	H	OCl	3.72

Legend: Fn – functional group

Molecular Docking and Drug-Likeness of the Analogs

Out of 232 analogs, 56 have better binding scores than the parent compounds across all target neuroreceptors with only two of them: (1) PTN_A Berbamine (PubChem ID: 275182) and (2) CDN_A (PubChem ID: 82279678) previously reported. The novel analogs were then assessed for drug-likeness based on the Lipinski filter's rule of five (Ro5) of SwissADME.

Most CDN_A and OSN_A did not violate the Ro5 owing to their smaller structure, while the analogs of bulkier bisbenzylisoquinoline alkaloids LMN, OMD, PTN, and PTR missed the MW cutoff (> 500) as expected. Natural compounds and their derivatives typically display two or more Ro5 violations; this has been seen with naturally derived alkaloids (e.g., bromocriptine and reserpine) and antimicrobials. Meanwhile, synthetic small-molecule drugs intended for oral delivery but with two or more Ro5 violations are not pursued in drug development [19]. Therefore, in this study, the analogs are considered drug-like if they have no more than 1 Ro5 violation. In total, 50 analogs (13 CDN_A, 2 LMN_A, 27 OSN_A, 2 OMD_A, 3 PTN_A, and 3 PTR_A) are novel and have predicted drug-likeness.

The mean absolute difference between the docking scores of each analog and their corresponding parent compound across all neuroreceptors was calculated to determine the molecular replacements that led to the highest improvement in docking score per alkaloid type. In the case of the bisbenzylisoquinoline alkaloids (BBIAs), replacement of the methoxy groups ($-OCH_3$) attached to the aromatic ring of the benzylisoquinoline moiety generally led to the improvement of docking scores. Some bioisosteres employed in this paper, such as isopropyl and methyl substitution of methoxy groups, were reported to increase the bioactivity against serotonin and G-protein coupled receptors in past studies [20-22]. Simple classical and non-classical substitutions in this paper also led to scoring improvements. For example, the substitution of methyl or hydrogens attached to the N-membered ring of the BBIAs with an alcohol group (-OH) as in the case of **3** follows Grimm's Hydride Displacement Law. Meanwhile, $-CH_2-$, -O-, -S- are considered non-classical bioisosteres that are useful heterocyclic replacements as in the case of 16 and 21 [23, 24].

Predicted pK Properties of Novel Strong-Binding Analogs of P. Ophthalmicus Alkaloids

For an oral drug to distribute and act in the CNS, it must be moderately polar and relatively lipophilic to achieve high passive human gastrointestinal absorption (GIA) and blood-brain barrier (BBB) permeability. It should also not be a substrate of the efflux transporter P-glycoprotein (P-gp) to maximize its entry across the BBB and must not inhibit the CYP1A2, CYP2C19, CYP2C9, CYP2D6, CYP3A4 to avoid pharmacokinetics-related drug-drug interactions [25, 26].

In this study, all ligands except PTR_A showed high GI absorption while most CDN_A and OSN_A were projected to be BBB permeable. Interestingly, the OMD_A and PTN_A improved the BBB permeability of their parent compounds. It was also predicted that the majority of CDN, LMN, OMD, and PTN analogs are not P-gp substrates in contrast to OSN, PTR, and their analogs. Favorable pK properties (high GIA, BBB permeable, non-P-gp substrate, and non-CYP isozyme inhibitor) were predicted for CDN_A 1, 3, and 5 with 3 being a highly promising oral neuropharmacological agent after exhibiting the best BE score among the CDN analogs across all target neuroreceptors as well.

Ligand Interactions of the Top Analogs

Hydrogen bonds are the prevailing directional intermolecular interactions in biological complexes and predominantly contribute to the specificity of molecular recognition. Aromatic interactions, on the other hand, are crucial to protein-ligand interaction and drug design by increasing the binding affinity of the inhibitor to its target but too many aromatic rings can also

adversely affect the physicochemical properties (e.g., solubility) of a drug candidate. Cation interactions are involved in the recognition of ACh by the nicotinic acetylcholine receptor (nAChR), as well as the receptors for GABA, glycine, and serotonin (5-HT) with their respective neurotransmitters [27].

For conciseness, only the interactions between 6G79 and 4MF3 and the top 3 performing analogs (across all neuroreceptors) per alkaloid type are covered here. Analog 3 is discussed due to its promising *in silico* activity and predicted pK. The molecular docking information (limited to H-bonding) and 2D interactions are shown in **Tables 4 and 5**, respectively.

Table 4. Molecular docking information of the top analogs

4MF3				
Analog	**Docking score (kcal/mol)**	**No of H-bonds**	**Interacting residues of the active site**	**H-bond length**
3	-6.08	3	T91	2.15, 2.65, 2.69
9	-5.86	3	T91	3.44
			R96	3.39
			E14	1.44
13	-5.86	3	S194	2.53
			E191	2.93, 2.92
14	-9.18	6	E191	3.17
			S174	2.08
			Y217	2.44
			S142	3.17
			T143	4.03
			S194	3.18
15	-8.55	4	R96	3.07
			K61	2.74
			G141	2.88, 3.68
16	-10.37	8	S174	2.89
			E14	1.75
			P89	2.70
			E191	2.41
			T143	2.84, 2.81
			S142	2.83
			M190	4.02
17	-10.64	5	T91	3.32
			G14	1.38
			L189	3.07
			E14	2.58, 2.95
21	-7.83	6	E191	3.31
			R96	3.79, 3.76
			T143	2.8
			S194	2.82
			S142	4.5
22	-8.01	1	R96	3.7
27	-8.27	7	S142	2.93, 2.80, 4.23
			Y217	2.76
			S194	2.60, 2.89, 2.78
33	-8.37	6	V138	2.76
			S142	3.01, 2.81, 3.14
			T143	3.03, 3.33
45	-10.4	9	T143	2.76
			L189	2.84
			Y217	2.54
			P89	2.72
			S174	2.8, 2.94, 3.03
			E14	2.66
			S142	4.09
46	-10.11	8	E191	3.13, 2.62
			T143	2.77
			E14	2.96
			P89	2.64
			E15	2.59
			S174	2.75, 3.27
47	-9.59	2	E14	2.92
			S142	4.13
48	-9.96	5	T143	2.85
			S142	3.12

			V138	3.09, 2.72
			P89	1.82
49	-11.13	10	T91	3.27, 3.06
			E14	2.89, 2.62
			E15	3.04
			G60	3.06, 2.72
			Y62	4.16
			S194	3.60, 3.58
50	-12.37	9	V138	3.29
			S174	3.33, 3.02, 3.64
			L189	2.66
			E14	2.88
			Y62	2.67
			T143	3.03

5O8F

Analog	Docking score (kcal/mol)	No of H-bonds	Interacting residues of the active site	H-bond length
3	-5.58	3	W249	2.92
			Q245	2.22
			I242	2.44
9	-5.14	2	Q245	2.88
			T309	2.67
13	-5.14	4	W249	3.27
			T309	2.30, 2.72
			Q245	2.83
14	-8.93	4	Y312	1.88, 3.10
			T309	3.27, 3.24
15	-9.1	0	N/A	N/A
16	-10.26	3	Q245	2.56
			R399	2.82
			T309	2.7
17	-9.9	2	W249	3.28
			Q245	2.75
21	-7.58	0	N/A	
22	-7.15	1	W249	3.31
27	-6.85	3	I242	2.28
			R399	2.47, 2.64
33	-6.95	3	I242	2.55
			R399	2.79
45	-11.33	4	W249	3.11
			R399	2.84
			E245	2.77
			T309	4.02
46	-9.71	3	W249	3.21
			T309	2.74
			P403	2.77
47	-9.11	2	Y312	2.72
			T309	3.84
48	-10.74	3	W249	2.84
			E245	1.89
			R399	2.14
49	-10.29	2	Q245	2.41
			I305	3.53
50	-10.2	1	T309	2.68

6G79

Analog	Docking score (kcal/mol)	No of H-bonds	Interacting residues of the active site	H-bond length
3	-7.24	3	A216	2.36
			D129	2.78
			T134	1.87
9	-6.52	6	T134	2.68, 3.31
			D129	1.31, 2.76

			S212	2.55, 2.53
13	-6.69	5	T134 S212 Y359 D129	1.94 2.80 2.47 2.41, 2.34
14	-9.18	6	P338 V201 T203	1.89, 2.3, 2.71 2.73 2.89
15	-7.3	1	Y109	2.71
16	-11.6	7	T209 F330 S334 N202 D129 S212	2.85 2.53 2.63 2.37 2.53 2.71, 3.09
17	-12.79	12	T134 D129 T203 V201 Y109 I30 T213 S334 Y359 V201	2.80, 3.03, 2.83 1.84 2.14 2.74 2.64 3.03 2.79 1.88 2 3.82
21	-9.23	2	Y359 T134	2.92 2.35
22	-9.2	0	N/A	
27	-8.32	4	Y359 S212 T134	2.75 2.54, 2.69 2.90
33	-8.96	4	Y359 S212 T134	2.86 2.54, 2.67 2.53
45	-12.2	5	D129 T203 L348 Y109	2.37, 2.72 3.04 2.68 3.65
46	-10.81	8	Y109 M337 I333 N202 S334 S212	2.70 2.73 2.64 3.09, 2.68 2.55 2.37, 3.52
47	-9.24	7	T209 M337 I333 N202 S334 S212	3.13 2.55 2.52 2.63, 2.49 2.57 2.40
48	-11.05	7	F346 P338 D129 L126 S334 T209 T203	2.48 2.37 2.19 2.56 2.60 2.74 4.16
49	-12.41	10	Y109 Y359 T355 D129 T134 S212 S334	2.96, 2.58 2.56 2.75 2.30 2.70 3.08, 2.50, 2.23 3.78
50	-12.82	7	W345	2.75, 2.70

			T203	3.36
			N202	2.66
			P338	3.03
			S334	3.53
			T209	4.09

6HUK				
Analog	**Docking score (kcal/mol)**	**No of H-bonds**	**Interacting residues of the active site**	**H-bond length**
3	-6.55	5	F46	3.39
			T202	3.19
			D44	2.21
			F66	3.49
			T130	3.47
9	-6.66	6	R67	3.06, 2.68
			Y97	2.59, 2.78
			E155	1.85
			Y157	2.76
13	-6.63	3	R207	2.81
			Y97	2.43
			Y157	1.82
14	-10.27	4	R67	2.77
			R177	3.17
			A201	3.16
			V199	2.48
15	-10.23	2	R67	2.69
			A201	3.37
16	-12.66	3	W65	2.68
			Y97	2.74
			R207	3.47
17	-11.45	3	R67	3.12
			R173	3.78
			W65	2.59
21	-8.84	2	Y205	3.28
			D44	2.78
22	-9.07	4	Y97	2.78
			Y157	2.56, 3.01
			E155	2.96
27	-9.11	6	Y97	2.68, 2.62
			F65	2.16
			S156	2.52
			Y157	2.29
			E155	2.01
33	-9.08	6	Y97	2.72, 2.63
			F65	2.14
			S156	2.58
			Y157	2.36
			E155	1.98
45	-11.51	9	A201	3.33, 4.18
			D44	2.21
			V199	2.74
			E183	2.57, 2.59
			W65	2.83, 2.99
			Y97	2.71
46	-10.86	2	R67	2.77
			T202	3.34
47	-11.72	5	R67	3.09
			Y157	2.29, 2.89
			Y97	2.52
			R207	4.15
48	-13.17	2	W65	2.02
			D44	2.71
49	-13.04	8	R67	3.18
			T202	3.26, 2.73
			Y205	3.13

			R207	3.16
			E183	2.38
			Y97	2.46
			E155	2.83
			Y97	2.68
50	-13.09	3	A201	2.95
			Y157	2.43

Table 5. 2D diagram of ligand interactions between the top analogs and target neuroreceptors

Analog	4MF3	5O8F	6G79	6HUK
3	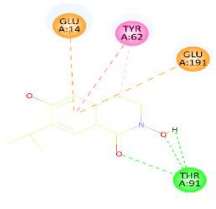	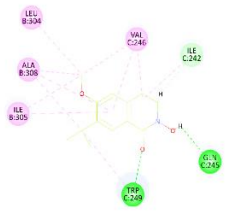	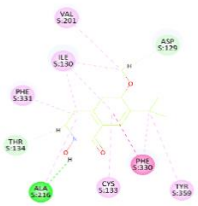	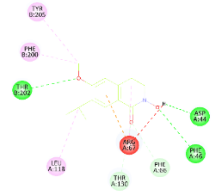
9	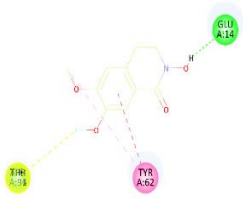	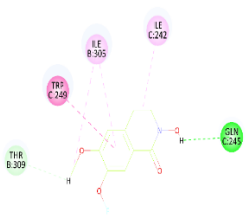	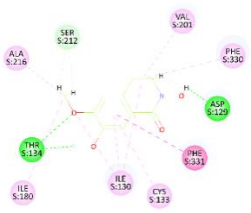	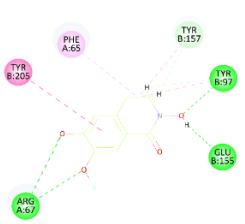
13	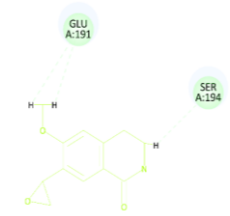	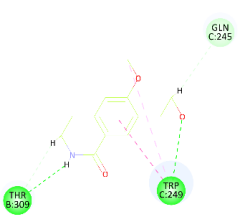	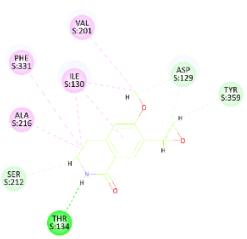	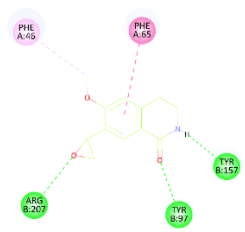
14	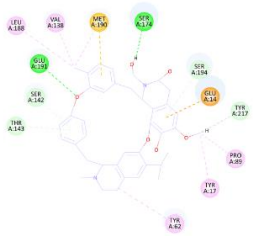	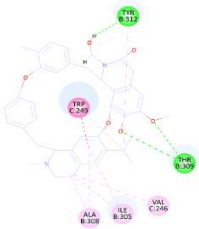	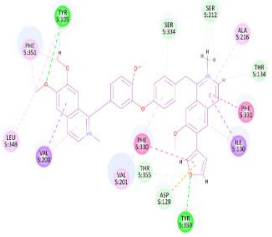	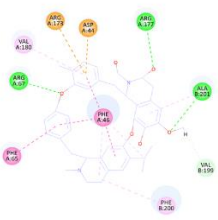
15	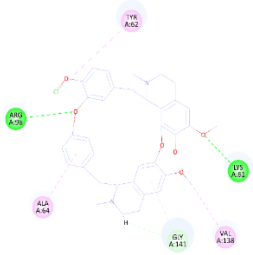	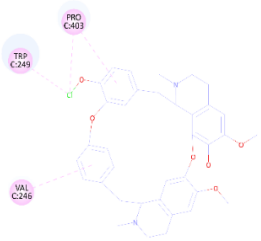	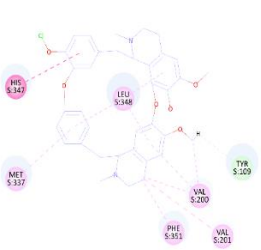	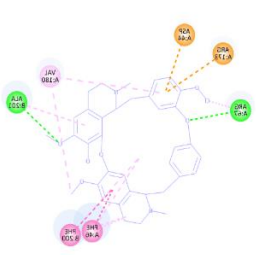

16	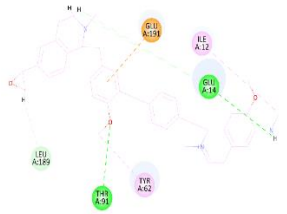	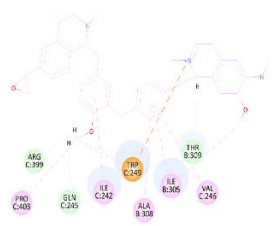	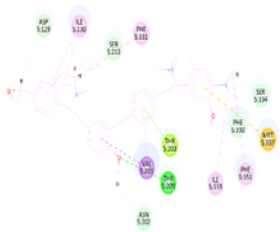	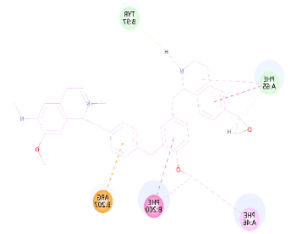
17	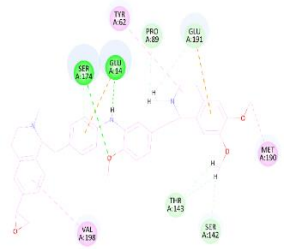	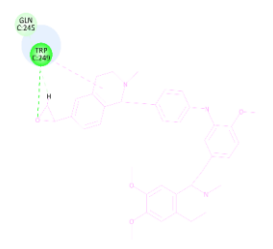	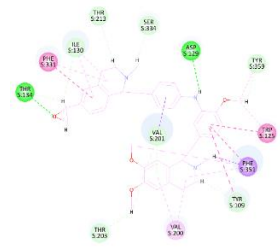	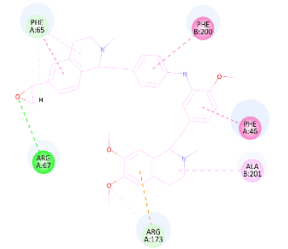
21	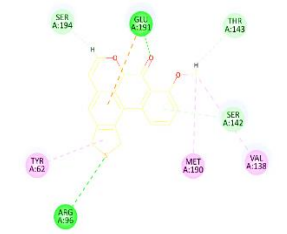	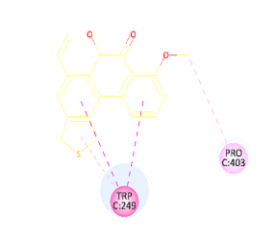	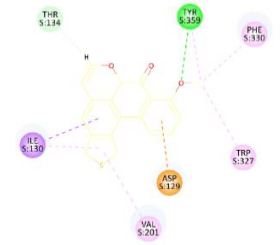	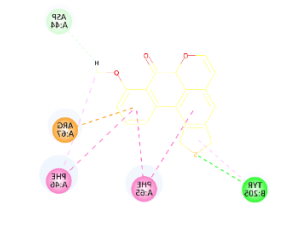
22		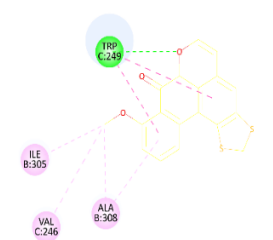	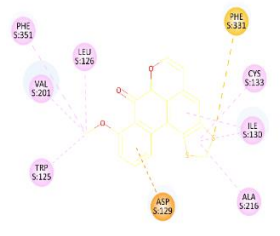	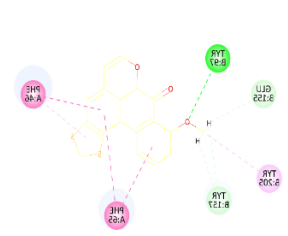
27	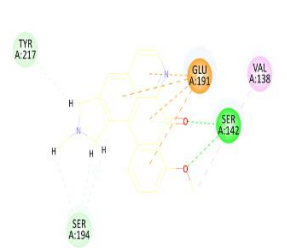	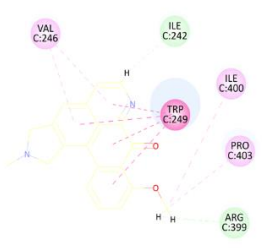	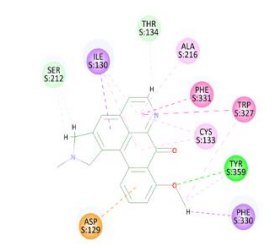	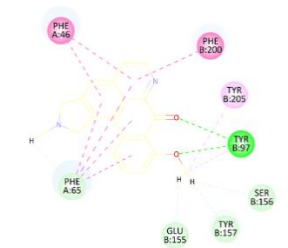
33	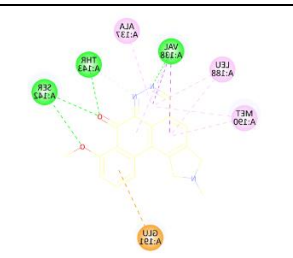	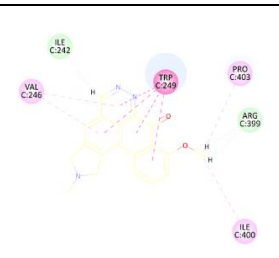	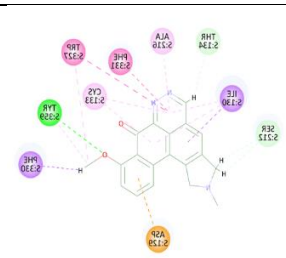	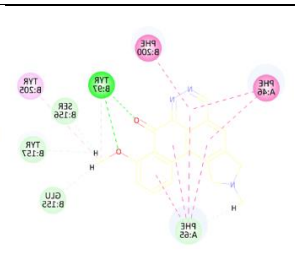

45	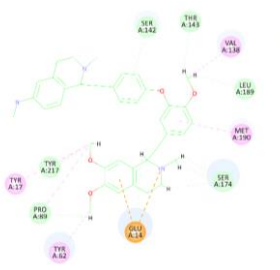	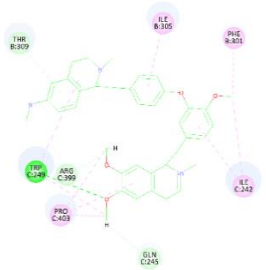	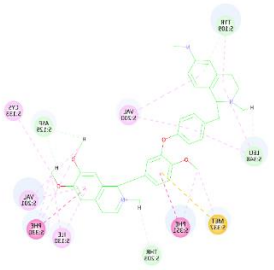	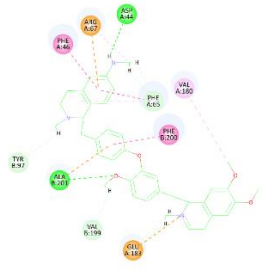
46	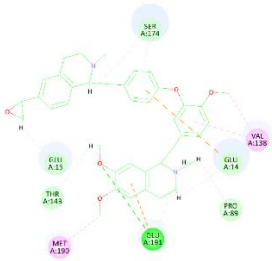	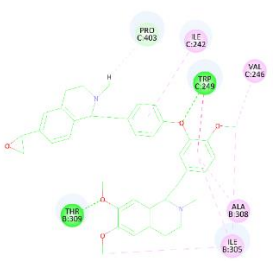	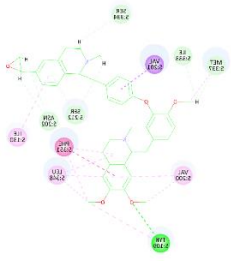	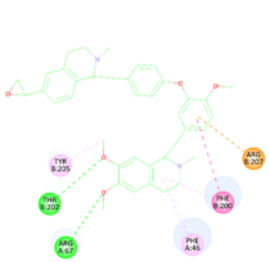
47	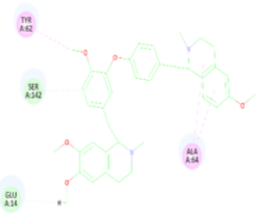	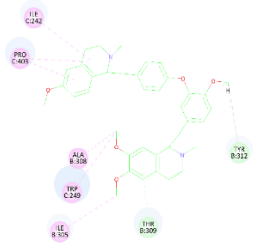	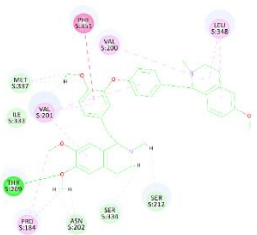	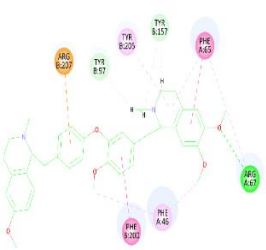
48	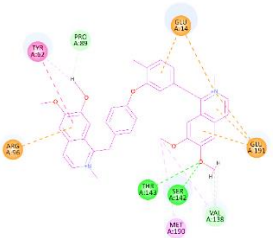	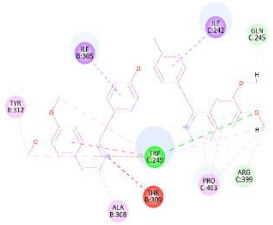	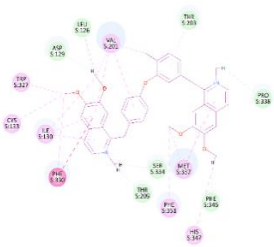	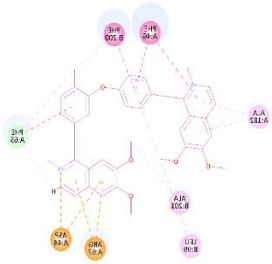
49	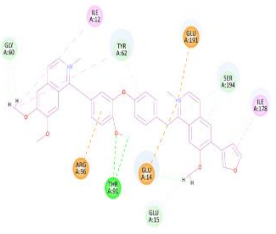	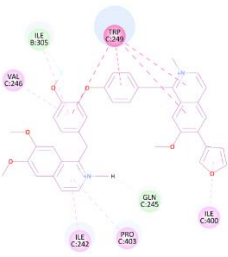	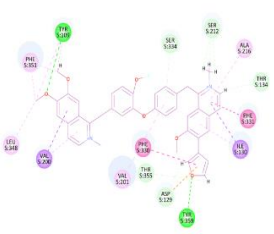	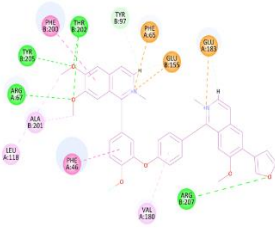
50	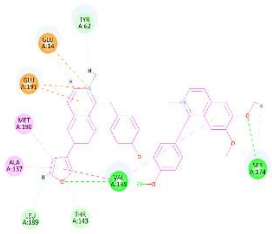	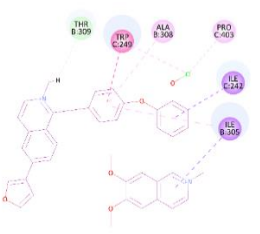	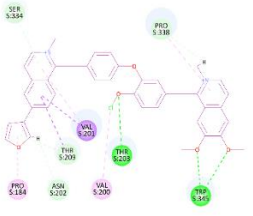	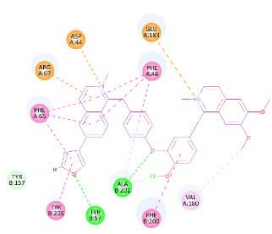

Key Binding Interactions with 6G79: 5-HT$_{1B}$ Receptor

The ligands ergotamine, donitriptan, and SB-236057 are known to interact with 5-HT$_{1B}$ receptor's orthosteric binding pocket residues D129, I130, C133, T134, Y208, S212, A216, W327, F330, F331, Y359; and W125, L126, V200, V201, T203, T209, S334, M337, F351, D352, T355 in the extended binding pockets [28-31].

Overall, 50 (PTR$_A$), 17 (OMD), and 49 (PTR$_A$) performed best with docking scores -12.82, -12.41, and -12.79 kcal/mol, respectively. The furan-substituted benzylisoquinoline ring of 50 was buried partially in the pocket while its other benzylisoquinoline ring protruded outside the cavity where it was held by residues W345 and P338 via H-bonds and hydrophobic contacts. Interestingly, by simply replacing PTR's methoxy group at C12 with a methyl (giving rise to 48), the analog had 4 more interactions and a shorter average H-bond distance. However, compared to 50, the average bond distance of 48 (-11.05 kcal/mol) is longer while the rest of its interactions are weaker hydrophobic contacts which could explain its higher BE score. Meanwhile, OMD$_A$ 16 and 17's oxirane moiety occupied the deeper part of the binding site, with 17 (-12.79 kcal/mol) having a lower BE score than 16 (-11.6 kcal/mol) due to the presence of more H-bonding and hydrophobic interactions at closer distances.

The top CDN$_A$ made 10 to 13 interactions with the residues in the orthosteric binding pocket and one in the extended binding pocket of 6G79. H-bonding and hydrophobic bonding accounted for most of these interactions, while in the case of 3 (BE: -7.24 kcal/mol), an additional pi-sulfur bond was formed with C133. It can be observed that 3, which outperformed 9 (-6.52 kcal/mol) and 13 (-6.69 kcal/mol), is buried deeper in the binding pocket than the other two.

Key Binding Interactions with 4MF3: Gluk1 Receptor

The top performing analogs of 4MF3 are 50, 49, and 17 with scores of -12.37, -11.13, and -10.64 kcal/mole, respectively. In the 4MF3 binding pocket, CDN$_A$ 3 and 9 occupied the same box lined by residues T91, R96, Y62, and E14, with E191 forming an additional electrostatic interaction with 3's benzene ring. This additional bond may have contributed to a slight improvement in the score of 3 (-6.08 kcal/mol) versus 9 (-5.86 kcal/mol).

OMD$_A$ 17 (cyan; BE: -10.64 kcal/mol) and 16 (orange; BE: -10.37 kcal/mol) have different conformations: 17 has an extended pose with its oxirane moiety stretched to the exterior of the cavity whereas 16 is folded in the hydrophobic pocket with its oxirane interacting with L189 via H-bond (other interacting residues: E191 and T91). The stretched conformation of 17 allowed contact to more residues lining the pocket (a total of 9) compared to 16's closed conformation where only 6 residues were seen to interact.

As for PTR and its analogs **(Figure 2)**, the presence of only one ether bridge connecting the benzyl rings provided the two isoquinoline moieties with more mobility inside the binding pocket. In general, one will notice that the more "squared out" the structure is — it assumes a square conformation with a spacious center — the better the score becomes. The researchers attributed this to two possible reasons: (1) a squared conformation means the isoquinoline/benzene rings can lay flat on the wide pocket floor, and (2) a spacious center reflects the ability of the structure to extend towards the sides of the cavity thus making more contact with residues lining the pocket. The analogs occupied the core of the 4MF3 pocket in different conformations, with the order of their BE scores increasing as follows: 50>49>48 (-12.37, -11.13, -9.96 kcal/mol).

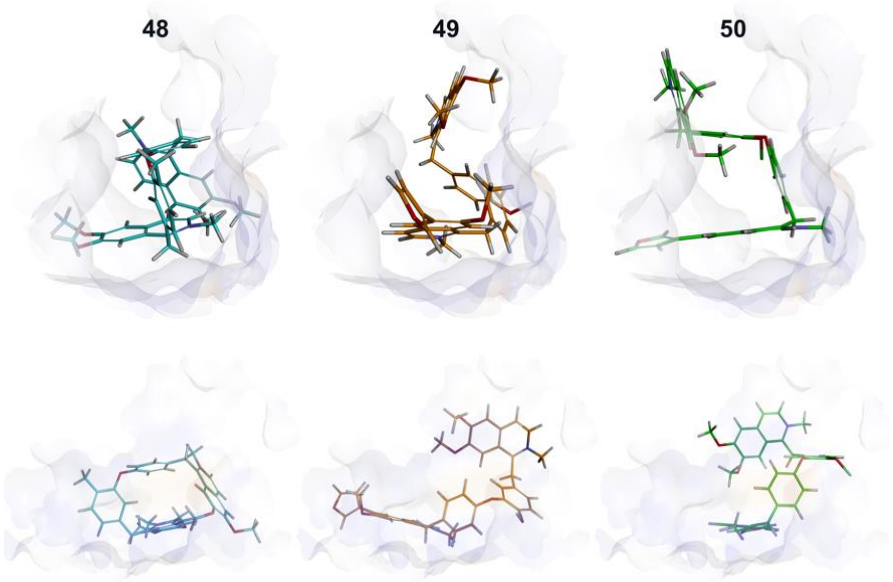

Figure 2. (Top pane) Front-view showing the triangle-like shape of the 4MF3 binding cavity with a wider base. (Bottom pane) Side-view orientation of the PTR ligands 48 (cyan), 49 (orange), and 50 (green) inside the said pocket.

The modifications in 50 are its furan ring at C6' and the removal of methoxy at C7', while 49 also has a furan ring but with the methoxy group retained at C7' (the carbon adjacent to the furan-containing carbon). With 50 outperforming 49, this suggests that the removal of the methoxy group is necessary for a better fit in the small pocket where the quaternary nitrogen of 50 was able to form attractive charges with E191 and E14 at shorter distances as well. Meanwhile, the 8 intramolecular bonds in 48 resulted in its folded form which led to 16 interactions only, the majority of which are electrostatically followed by H-bond.

Conclusion

Recent studies on *P. ophthalmicus* confirmed some of its ethnomedicinal uses which were attributed to alkaloids (+)-tetrandrine and limacusine. It also contains phaeantharine, phaeanthine, oxostephanine, and *O*-methyldauricine, which are alkaloids containing a benzylisoquinoline moiety also present in the known neuroactive drugs papaverine, morphine, and tubocurarine. Molecular docking is a widely accepted tool for drug discovery and drug repurposing where new indications for existing drug candidates could be explored at a lower cost similar to high-performance biological screening.

As of this writing, there have been no investigations into the neuropharmacological uses of these alkaloids yet; therefore, extensive molecular docking studies were performed. Our results identified 4MF3 (Kainate 1), 5O8F and 6HUK ($GABA_A$), and 6G79 (Serotonin 1B) as potential neuroreceptor targets which are involved with pain, migraine, stroke, epilepsy, and anxiety, among other neurological disorders.

In addition, ligand modifications were done to improve the *in silico* binding activity and properties of these compounds. Replacement of the methoxy groups ($-OCH_3$) attached to the aromatic ring of the benzylisoquinoline moiety generally led to the improvement of docking scores. Heterocyclic replacements as in the case of 16 and 21 proved to be beneficial as well. In total, 50 analogs (13 CDN, 2 LMN, 27 OSN, 2 OMD, 3 PTN, and 3 PTR) were considered promising neuropharmacological agents after displaying better docking scores, novelty, and predicted drug-likeness. One particular CDN_A (3), 2,6-dihydroxy-7-(propan-2-yl)-1,2,3,4-tetrahydroisoquinolin-1-one, is considered a very promising oral neuropharmacological agent after displaying consistent top docking scores across all neuroreceptors while also having a favorable pK and drug-likeness *in silico*. Therefore, the synthesis of 3 and investigation of its *in vitro* and *in vivo* activity are highly suggested by the researchers. Additional molecular dynamics simulations for the top analogs are also recommended to provide more details on the dynamic performance of ligand-receptor interactions such as binding stability.

Acknowledgments: The valuable contributions of Dr. Salvador Eugenio C. Caoili, Prof. Joanna V. Toralba, Prof. Vince Lambert H. Padilla, and Mr. Thomas Lemker to this study are greatly acknowledged.

Conflict of interest: None

Financial support: This study was funded under the Accelerated Science and Technology Human Resource Development Program of the Department of Science and Technology (ASTHRDP-DOST), Philippines.

Ethics statement: None

References

1. Avan A, Hachinski V. Stroke and dementia, leading causes of neurological disability and death, the potential for prevention. Alzheimers Dement. 2021;17(6):1072-6. doi:10.1002/alz.12340
2. Feigin VL, Nichols E, Alam T, Bannick MS, Beghi E, Blake N, et al. Global, regional, and national burden of neurological disorders, 1990–2016: a systematic analysis for the Global Burden of Disease Study 2016. Lancet Neurol. 2019;18(5):459-80. doi:10.1016/S1474-4422(18)30499-X
3. Atan MS, Dzulkefly KA, Mohd Aspollah S, Anuar K, Vijay S. Isolation and Antibacterial Activity of Alkaloids from Phaeanthus opthalmicus. Asian J Chem. 2011;23(9):3824-6.
4. Magpantay HD, Malaluan IN, Manzano JAH, Quimque MT, Pueblos KR, Moor N, et al. Antibacterial and COX-2 Inhibitory Tetrahydrobisbenzylisoquinoline Alkaloids from the Philippine Medicinal Plant Phaeanthus ophthalmicus. Plants. 2021;10(3):462. doi:10.3390/plants10030462
5. Malaluan IN, Manzano JAH, Muñoz JER, Bautista TJL, Dahse HM, Quimque MTJ, et al. Antituberculosis and Antiproliferative Activities of the Extracts and Tetrahydrobisbenzylisoquinoline Alkaloids from Phaeanthus ophthalmicus: In Vitro and Silico Investigations. Philipp J Sci. 2022;151(1):371-81.
6. Cabedo N, Berenguer I, Figadere B, Cortes D. An Overview on Benzylisoquinoline Derivatives with Dopaminergic and Serotonergic Activities. Curr Med Chem. 2009;16(19):2441-67. doi:10.2174/092986709788682100
7. Singla D, Sharma A, Kaur J, Panwar B, Raghava GP. BIAdb: A curated database of benzylisoquinoline alkaloids. BMC Pharmacol. 2010;10(1):1-8.
8. Li Y, Guo B, Xu Z, Li B, Cai T, Zhang X, et al. Repositioning organohalogen drugs: a case study for identification of potent B-Raf V600E inhibitors via docking and bioassay. Sci Rep. 2016;6(1):31074. doi:10.1038/srep31074

9. Anukanon S, Pongpamorn P, Tiyabhorn W, Chatwichien J, Niwetmarin W, Sessions RB, et al. In Silico-Guided Rational Drug Design and Semi-synthesis of C(2)-Functionalized Huperzine A Derivatives as Acetylcholinesterase Inhibitors. ACS Omega. 2021;6(30):19924-39. doi:10.1021/acsomega.1c02875
10. Gnanaraj C, Sekar M, Fuloria S, Swain SS, Gan SH, Chidambaram K, et al. In Silico Molecular Docking Analysis of Karanjin against Alzheimer's and Parkinson's Diseases as a Potential Natural Lead Molecule for New Drug Design, Development and Therapy. Molecules. 2022;27(9):2834. doi:10.3390/molecules27092834
11. Billones JB, Bangalan MAT. Structure-Based Discovery of Inhibitors Against MurE in Methicillin-Resistant Staphylococcus Aureus. Orient J Chem. 2019;35(2):618-25. doi:10.13005/ojc/350216
12. Wang S, Jiang JH, Li RY, Deng P. Docking-based virtual screening of TβR1 inhibitors: evaluation of pose prediction and scoring functions. BMC Chem. 2020;14(1):52. doi:10.1186/s13065-020-00704-3
13. Ramírez D, Caballero J. Is It Reliable to Take the Molecular Docking Top Scoring Position as the Best Solution without Considering Available Structural Data? Molecules. 2018;23(5):1038. doi:10.3390/molecules23051038
14. Wirth M, Zoete V, Michielin O, Sauer WHB. SwissBioisostere: A database of molecular replacements for ligand design. Nucleic Acids Res. 2013;41(D1):1137-43. doi:10.1093/nar/gks1059
15. Daina A, Zoete V. Application of the SwissDrugDesign Online Resources in Virtual Screening. Int J Mol Sci. 2019;20(18):4612. doi:10.3390/ijms20184612
16. Masiulis S, Desai R, Uchański T, Serna Martin I, Laverty D, Karia D, et al. GABAA receptor signaling mechanisms revealed by structural pharmacology. Nature. 2019;565(7740):454-9. doi:10.1038/s41586-018-0832-5
17. Cuozzo A, Daina A, Perez MAS, Michielin O, Zoete V. SwissBioisostere 2021: updated structural, bioactivity and physicochemical data delivered by a reshaped web interface. Nucleic Acids Res. 2022;50(D1):D1382-90. doi:10.1093/nar/gkab1047
18. Tse EG, Houston SD, Williams CM, Savage GP, Rendina LM, Hallyburton I, et al. Nonclassical Phenyl Bioisosteres as Effective Replacements in a Series of Novel Open-Source Antimalarials. J Med Chem. 2020;63(20):11585-601. doi:10.1021/acs.jmedchem.0c00746
19. Benet LZ, Hosey CM, Ursu O, Oprea TI. BDDCS, the Rule of 5, and drugability. Adv Drug Deliv Rev. 2016;101:89-98. doi:10.1016/j.addr.2016.05.007
20. Leopoldo M, Lacivita E, de Giorgio P, Fracasso C, Guzzetti S, Caccia S, et al. Structural Modifications of N -(1,2,3,4-Tetrahydronaphthalen-1-yl)-4-Aryl-1-piperazinehexanamides: Influence on Lipophilicity and 5-HT 7 Receptor Activity. Part III. J Med Chem. 2008;51(18):5813-22. doi:10.1021/jm800615e
21. Ivachtchenko AV, Golovina ES, Kadieva MG, Koryakova AG, Kovalenko SM, Mitkin OD, et al. Synthesis and biological study of 3-(phenylsulfonyl)thieno[2,3-e][1,2,3]triazolo[1,5-a]pyrimidines as potent and selective serotonin 5-HT6 receptor antagonists. Bioorg Med Chem. 2010;18(14):5282-90. doi:10.1016/j.bmc.2010.05.051
22. Zheng G, Smith AM, Huang X, Subramanian KL, Siripurapu KB, Deaciuc A, et al. Structural Modifications to Tetrahydropyridine-3-carboxylate Esters en Route to the Discovery of M 5 -Preferring Muscarinic Receptor Orthosteric Antagonists. J Med Chem. 2013;56(4):1693-703. doi:10.1021/jm301774u
23. Dick A, Cocklin S. Bioisosteric Replacement as a Tool in Anti-HIV Drug Design. Pharmaceuticals (Basel). 2020;13(3):36. doi:10.3390/ph13030036
24. Meanwell NA. The influence of bioisosteres in drug design: tactical applications to address developability problems. InTactics in Contemporary Drug Design 2013 (pp. 283-381). Springer, Berlin, Heidelberg. doi:10.1007/7355_2013_29
25. Finch A, Pillans P. P-glycoprotein and its role in drug-drug interactions. Aust Prescr. 2014;37(4):137-9. doi:10.18773/austprescr.2014.050
26. Daina A, Michielin O, Zoete V. SwissADME: A free web tool to evaluate pharmacokinetics, drug-likeness and medicinal chemistry friendliness of small molecules. Sci Rep. 2017;7(1):1-13. doi:10.1038/srep42717
27. Ferreira de Freitas R, Schapira M. A systematic analysis of atomic protein-ligand interactions in the PDB. Medchemcomm. 2017;8(10):1970-81. doi:10.1039/C7MD00381A
28. García-Nafría J, Nehmé R, Edwards PC, Tate CG. Cryo-EM structure of the serotonin 5-HT1B receptor coupled to heterotrimeric Go. Nature. 2018;558(7711):620-3. doi:10.1038/s41586-018-0241-9
29. Wang C, Jiang Y, Ma J, Wu H, Wacker D, Katritch V, et al. Structural basis for molecular recognition at serotonin receptors. Science. 2013;340(6132):610-4. doi:10.1126/science.1232807
30. Wang Y, Lin W, Wu N, Wang S, Chen M, Lin Z, et al. Structural insight into the serotonin (5-HT) receptor family by molecular docking, molecular dynamics simulation and systems pharmacology analysis. Acta Pharmacol Sin. 2019;40(9):1138-56. doi:10.1038/s41401-019-0217-9
31. Xu P, Huang S, Zhang H, Mao C, Zhou XE, Cheng X, et al. Structural insights into the lipid and ligand regulation of serotonin receptors. Nature. 2021;592(7854):469-73. doi:10.1038/s41586-021-03376-8